

An efficient algorithm for weakly compressible flows in spherical geometries

Roman Frolov^a, Peter Minev^a, Aziz Takhirov^a

^a*Department of Mathematical and Statistical Sciences, University of Alberta, Edmonton, AB, T6G 2G1, Canada*

Abstract

This study proposes an algorithm for modeling compressible flows in spherical shells in nearly incompressible and weakly compressible regimes based on an implicit direction splitting approach. The method retains theoretically expected convergence rates and remains stable for extremely small values of the characteristic Mach number (at least as low as $M_0 = 10^{-6}$). The staggered spatial discretization on the MAC stencil, commonly used in numerical methods for incompressible Navier-Stokes equations, was found to be convenient for the discretization of the compressible Navier-Stokes equations written in the non-conservative form in terms of the primitive variables. This approach helped to avoid the high-frequency oscillations without any artificial stabilization terms. Nonlinear Picard iterations with the splitting error reduction were also implemented to allow one to obtain a solution of the fully nonlinear system of equations. These results, alongside excellent parallel performance, prove the viability of the direction splitting approach in large-scale high-resolution high-performance simulations of atmospheric and oceanic flows.

Keywords: Splitting methods, compressible Navier-Stokes equations on the sphere, Parallel algorithm.

1. Introduction.

The main motivation for this study comes from the atmospheric science and oceanography, where reliable dynamical cores for global and local ocean-atmosphere circulations are required to decrease uncertainties in numerical weather prediction, ocean circulation, and climate modelling. Despite the rapid advance in numerical methods for atmospheric and oceanic flows, there are still several important challenges remaining in this field. Among them are the need to avoid simplifications of the model that may only be valid in certain asymptotic limits, improve the efficiency and increase the accuracy and resolution of the computations while maintaining stability, consistently couple ocean and atmosphere models together, and many others.

Very generally speaking, the atmospheric and ocean models can be divided into two large classes: hydrostatic and non-hydrostatic. In the first case the flow in the vertical direction is "homogenized" based on the assumption that the spherical shell domain of the flow is very thin as compared to its size in the other directions, while in the second case the model explicitly involves in the system of equations the balance of mass, momentum, and energy in the vertical direction as well. Of course, the non-hydrostatic models are

Email addresses: frolov@ualberta.ca (Roman Frolov), pminev@ualberta.ca (Peter Minev), takhirov@ualberta.ca (Aziz Takhirov)

the most comprehensive models of the atmosphere and the oceans, and naturally, they are based on the 3D compressible Navier-Stokes equations. This system can be further enhanced by introducing equations accounting for the moisture content and pollutants in the atmosphere, salinity of the oceans, etc., thus enhancing the accuracy of the modelling effort, but also increasing the complexity of the PDE system, and the required computational effort for their numerical approximation. Therefore, until the appearance of the modern parallel computer systems, the hydrostatic approach was prevailing. However, in the last two decades, the modelling community clearly more and more often employs the complete 3D models. But even the 3D computational cores are often based on some simplified models like the compressible/incompressible Euler equations or the incompressible Boussinesq equations. The computational reason for considering the Euler equations is usually the fact that they can be efficiently discretized by means of fully explicit schemes while the incompressible models avoid the numerical difficulties related to the treatment of the weakly compressible flows. Excellent summaries of the present models in meteorology and climatology can be found in [1] and in oceanology - in [2]. These articles contain also numerous references to various modelling and computational efforts in these areas, and therefore we refer the reader to these references for obtaining a more complete picture of the state-of-the-art techniques for resolution of such models. Our effort in the present study is focussed on the development of an efficient parallel algorithm for the solution of the 3D weakly compressible Navier-Stokes equations in a spherical shell, using semi- or fully implicit schemes in time and a finite difference approximation in space. The main guidelines for the design of the algorithm were: (i) minimization of the computational effort; (ii) maximization of its parallel performance. Although we do not claim that we completely achieved those goals, we do believe that this study is a step in the right direction that will eventually lead to the ability to resolve the coupled ocean-atmosphere system with satisfactory resolution on the scale of the entire Earth. The discretization methodology in this study is applied to the compressible Navier-Stokes equations with the so-called Stiffened Gas (SG) equation of state in spherical coordinates. The advection terms are written in a non-conservative form, that in our opinion is more appropriate for weakly compressible flows. This set is further discretized implicitly using the Linearized-Block-Implicit (LBI) direction splitting scheme based on the second order Douglas splitting [3], that allows for a stable and cheap integration in time (see [4] and the references therein). In addition, it also allows for a very efficient parallelization if this time discretization is combined with a finite difference approximation in space. We use a staggered Marker-and-Cell (MAC) grid instead of the centred non-staggered discretization that is commonly employed in case of higher Mach numbers. This helps to avoid the high-frequency pressure oscillations without the introduction of any stabilization terms.

The rest of the paper is organized as follows. We describe the details of the proposed algorithm in Section 2. Numerical experiments are described in Section 3, and we provide some concluding remarks in Section 4.

2. Formulation and its discretization

The flows in the atmosphere and the ocean occur at extremely low to moderate values of the Mach number, and therefore no shock waves are observed in the solution. Hence, the non-conservative formulation with pressure p , velocity \mathbf{u} , and temperature T as unknowns is suitable for their description, since this is the most widely used setting in the incompressible regime. In case of dry, stratified air, it means solving the following system of PDEs (see Appendix A for a detailed derivation of this system based on the conservative equation set for atmospheric modelling from [1]¹):

$$\begin{aligned} \frac{\partial T}{\partial t} + \mathbf{u} \cdot \nabla T + (\gamma - 1)T \nabla \cdot \mathbf{u} - \frac{(\gamma - 1)T}{p + \pi_\infty} \nabla \cdot \left(\frac{\mu c_p}{Pr} \nabla T \right) \\ - \frac{(\gamma - 1)T}{p + \pi_\infty} \nabla \mathbf{u} : \hat{\boldsymbol{\sigma}} = 0, \end{aligned} \quad (2.1)$$

$$\frac{\partial \mathbf{u}}{\partial t} + \mathbf{u} \cdot \nabla \mathbf{u} + \frac{1}{\rho} \nabla p - \frac{1}{\rho} \nabla \cdot \hat{\boldsymbol{\sigma}} + \mathbf{g} + 2(\mathbf{u} \times \boldsymbol{\omega}) = 0, \quad (2.2)$$

$$\begin{aligned} \frac{\partial p}{\partial t} + \mathbf{u} \cdot \nabla p + \gamma(p + \pi_\infty) \nabla \cdot \mathbf{u} - (\gamma - 1) \nabla \cdot \left(\frac{\mu c_p}{Pr} \nabla T \right) \\ - (\gamma - 1) \nabla \mathbf{u} : \hat{\boldsymbol{\sigma}} = 0. \end{aligned} \quad (2.3)$$

where $\boldsymbol{\omega}$ is the rotational velocity of the Earth, $\hat{\boldsymbol{\sigma}}$ is the viscous stress tensor given by

$$\hat{\boldsymbol{\sigma}} = \mu \left[(\nabla \mathbf{u} + (\nabla \mathbf{u})^T) - \frac{2}{3} (\nabla \cdot \mathbf{u}) \hat{I} \right],$$

\mathbf{g} is the sum of the true gravity and the centrifugal force, c_p , c_v , μ , Pr , $\gamma = \frac{c_p}{c_v}$, π_∞ are constant for each material, and the density ρ is given by the Stiffened Gas Equation of State ([5]):

$$\rho = \frac{p + \pi_\infty}{c_v(\gamma - 1)T}. \quad (2.4)$$

The system (2.1)-(2.3) is considered in a part of a spherical shell given by:

$$\Omega := \left\{ (r, \theta, \phi) \in [R_1, R_2] \times \left[\frac{\pi}{4}, \frac{3\pi}{4} \right] \times \left[\frac{\pi}{4}, \frac{7\pi}{4} \right] \right\}.$$

Although it was not done in this study, the domain decomposition technique described in [6] can be employed to extend the domain to the whole spherical shell.

In order to simplify the notations, we denote the vector of unknowns as $\mathbf{U} = [p, u_r, u_\theta, u_\phi, T]^T$, the gravity vector as $\mathbf{G} = [0, \mathbf{g}^T, 0]^T$, and combine all the components of the differential operators in the corresponding directions into the $\mathbf{D}_r(\mathbf{U})$, $\mathbf{D}_\theta(\mathbf{U})$, and $\mathbf{D}_\phi(\mathbf{U})$ operators, and all the mixed derivatives, derivatives in staggered directions, and other terms not suitable for implicit treatment by the direction splitting approach into the $\mathbf{D}_M(\mathbf{U})$ operator (see (4.31), (4.32), (4.33), and (4.34) for definitions of these operators). Then the system (2.1)-(2.3) can be written in a compact form as (see Appendix C for details):

$$\frac{\partial \mathbf{U}}{\partial t} + \mathbf{D}_r(\mathbf{U})\mathbf{U} + \mathbf{D}_\theta(\mathbf{U})\mathbf{U} + \mathbf{D}_\phi(\mathbf{U})\mathbf{U} + \mathbf{D}_M(\mathbf{U})\mathbf{U} + \mathbf{G} = 0. \quad (2.5)$$

¹The system contains a dimensionless parameter, the Prandtl number Pr , as well as dimensional parameters. This is a somewhat unusual setting, introduced in [1] but for the sake of consistency with this publication we keep it here.

Using the Crank-Nicolson time-discretization strategy and the Picard iterations (see e.g. [7], Chapter 3), the semi-discrete version of (2.5) reads as:

$$\begin{aligned} \frac{\mathbf{U}_{k+1}^{n+1} - \mathbf{U}^n}{\tau} + \frac{1}{2} \mathbf{D}^{n+\frac{1}{2},(k)} \mathbf{U}_{k+1}^{n+1} + \frac{1}{2} \mathbf{D}^{n+\frac{1}{2},(k)} \mathbf{U}^n + \\ \frac{1}{2} \mathbf{D}_{\mathbf{M}}^{n+\frac{1}{2},(k)} \mathbf{U}_k^{n+1} + \frac{1}{2} \mathbf{D}_{\mathbf{M}}^{n+\frac{1}{2},(k)} \mathbf{U}^n + \mathbf{G} = 0, \end{aligned} \quad (2.6)$$

where

$$\begin{aligned} \mathbf{D}(U) &= \mathbf{D}_{\mathbf{r}}(\mathbf{U}) + \mathbf{D}_{\boldsymbol{\theta}}(\mathbf{U}) + \mathbf{D}_{\boldsymbol{\phi}}(\mathbf{U}), \\ \mathbf{D}^{n+\frac{1}{2},(k)} &= \mathbf{D} \left(\frac{\mathbf{U}_k^{n+1} + \mathbf{U}^n}{2} \right), \end{aligned}$$

τ is the time-step, subindex n refers to the time level, subindex k refers to the iteration level. From now on we skip the superscripts of operators for brevity, assuming that $\mathbf{D} = \mathbf{D}^{n+\frac{1}{2},(k)}$. Next, we approximate (2.6) by a Douglas-type (see [3]) direction splitting scheme that can be written in the following factorized form:

$$\begin{aligned} \left(I + \frac{\tau}{2} \mathbf{D}_{\mathbf{r}} \right) \left(I + \frac{\tau}{2} \mathbf{D}_{\boldsymbol{\theta}} \right) \left(I + \frac{\tau}{2} \mathbf{D}_{\boldsymbol{\phi}} \right) (\mathbf{U}_{k+1}^{n+1} - \mathbf{U}^n) = \\ -\tau \mathbf{D} \mathbf{U}^n - \tau \mathbf{G} - \frac{\tau}{2} \mathbf{D}_{\mathbf{M}} \mathbf{U}_k^{n+1} - \frac{\tau}{2} \mathbf{D}_{\mathbf{M}} \mathbf{U}^n. \end{aligned} \quad (2.7)$$

This splitting error reduction step can be combined with a Picard nonlinear iteration by adding

$$\begin{aligned} \mathbf{ER}(\mathbf{U}_k^{n+1} - \mathbf{U}^n) &= \left(I + \frac{\tau}{2} \mathbf{D}_{\mathbf{r}} \right) \left(I + \frac{\tau}{2} \mathbf{D}_{\boldsymbol{\theta}} \right) \left(I + \frac{\tau}{2} \mathbf{D}_{\boldsymbol{\phi}} \right) (\mathbf{U}_k^{n+1} - \mathbf{U}^n) - \\ &\quad \left(I + \frac{\tau}{2} \mathbf{D} \right) (\mathbf{U}_k^{n+1} - \mathbf{U}^n) \end{aligned}$$

to the right-hand-side of (2.7). After rearranging terms for convenience and computational efficiency, we obtain the following factorized direction splitting iteration to be solved until convergence:

$$\begin{aligned} \left(I + \frac{\tau}{2} \mathbf{D}_{\mathbf{r}} \right) \left(I + \frac{\tau}{2} \mathbf{D}_{\boldsymbol{\theta}} \right) \left(I + \frac{\tau}{2} \mathbf{D}_{\boldsymbol{\phi}} \right) (\mathbf{U}_{k+1}^{n+1} - \mathbf{U}_k^{n+1}) = \\ - \left(I + \frac{\tau}{2} \mathbf{D} \right) (\mathbf{U}_k^{n+1} - \mathbf{U}^n) - \tau \mathbf{D} \mathbf{U}^n - \tau \mathbf{G} \\ - \frac{\tau}{2} \mathbf{D}_{\mathbf{M}} \mathbf{U}_k^{n+1} - \frac{\tau}{2} \mathbf{D}_{\mathbf{M}} \mathbf{U}^n. \end{aligned} \quad (2.8)$$

This approach can also be viewed as a preconditioned Richardson iterative method. Note that, as a more accurate direction splitting method, the Douglas scheme has a $\mathcal{O}(\tau^2)$ splitting error, and therefore it is expected that this iteration would converge faster than an iteration based on a first-order direction splitting scheme. Furthermore, the splitting error reduction strategy described above has a computational complexity of the same order as the nonlinear Picard iterations without the splitting error reduction.

The system (2.8) can be solved as a sequence of three one-dimensional problems:

$$\left(I + \frac{\tau}{2}\mathbf{D}_r\right) (\boldsymbol{\xi}^{n+1} - \mathbf{U}_k^{n+1}) = \quad (2.9)$$

$$\begin{aligned} & - \left(I + \frac{\tau}{2}\mathbf{D}\right) (\mathbf{U}_k^{n+1} - \mathbf{U}^n) \\ & - \tau\mathbf{D}\mathbf{U}^n - \tau\mathbf{G} - \frac{\tau}{2}\mathbf{D}_M\mathbf{U}_k^{n+1} - \frac{\tau}{2}\mathbf{D}_M\mathbf{U}^n, \end{aligned}$$

$$\left(I + \frac{\tau}{2}\mathbf{D}_\theta\right) (\boldsymbol{\eta}^{n+1} - \mathbf{U}_k^{n+1}) = \boldsymbol{\xi}^{n+1} - \mathbf{U}_k^{n+1}, \quad (2.10)$$

$$\left(I + \frac{\tau}{2}\mathbf{D}_\phi\right) (\mathbf{U}_{k+1}^{n+1} - \mathbf{U}_k^{n+1}) = \boldsymbol{\eta}^{n+1} - \mathbf{U}_k^{n+1} \quad (2.11)$$

where $\boldsymbol{\xi}^{n+1}$, $\boldsymbol{\eta}^{n+1}$, and \mathbf{U}_{k+1}^{n+1} are subsequent approximations of the exact solution at t^{n+1} . Each of these problems requires a solution of a block-tridiagonal linear system only, which can be performed by the block-tridiagonal extension of the Thomas algorithm for tridiagonal systems (e.g. see [8], Volume 1, pp.188-189). The parallel implementation of the Thomas algorithm using the Schur complement technique and domain decomposition, as described in [9], can be easily extended for the block-tridiagonal version of the linear solver. Weak scalability results for the method can be found in [4].

Note that since a staggered discretization on the MAC stencil is employed, no artificial stabilization terms for the pressure are required.

3. Numerical tests.

The numerical experiments presented below confirm the accuracy of the proposed scheme in a wide range of Mach numbers ($M \in [10^{-6}, 10^{-1}]$), the correct behaviour of the numerical solution in the incompressible limit, and excellent parallel performance of the method.

3.1. Well-prepared manufactured solution.

The following manufactured solution has been used to verify the implementation and study the properties of the algorithm:

$$\begin{aligned} \rho &= \rho_0 = 1, \\ p &= p_0 + u_0^2 (1 + \sin(5t) + \cos^2(\pi r) \cos^2(4\phi) \cos^2(4\theta)), \\ u_r &= \frac{u_0(1 + \sin t)}{2r^2} + \frac{u_0^2}{c_0} (1 + \sin(4t) + \sin(r^2) \cos^3(\theta) \sin^2(\phi)), \\ u_\theta &= \frac{u_0(1 + \cos(3t + 2))}{2 \sin \theta} + \frac{u_0^2}{c_0} (1 + \sin(t) + \cos^3(r^2) \cos^2(\theta) \sin^3(\phi)), \\ u_\phi &= \frac{u_0(1 + \sin(6 + t))}{2} + \frac{u_0^2}{c_0} (1 + \cos(2 + t) + \cos(r) \sin^3(\theta) \sin^2(\phi)), \\ T &= \frac{p}{c_v(\gamma - 1)}. \end{aligned}$$

Note that this solution provides well-prepared initial data, i.e. it has the correct scaling with respect to the Mach number. Thus, it can be used to study the behaviour of the scheme in the incompressible ($M_0 \rightarrow 0$)

τ	$M_0 = 10^{-2}$	$M_0 = 10^{-4}$	$M_0 = 10^{-6}$
$2 \cdot 10^{-3}$	(1.8, 1.7)	(3.2, 3.2)	(3.2, 3.2)
$1 \cdot 10^{-3}$	(1.9, 1.9)	(2.7, 2.6)	(2.7, 2.5)
$5 \cdot 10^{-4}$	(1.9, 1.9)	(1.6, 1.5)	(1.4, 1.5)

Table 1: Order of time convergence for (p, T) computed using the inverse Richardson extrapolation approach.

τ	$M_0 = 10^{-2}$	$M_0 = 10^{-4}$	$M_0 = 10^{-6}$
2×10^{-3}	(2.3, 2.9, 2.6)	(3.2, 2.5, 2.9)	(2.5, 2.9, 2.4)
1×10^{-3}	(2.4, 2.7, 3.2)	(2.4, 2.8, 2.6)	(2.4, 2.8, 2.3)
5×10^{-4}	(2.1, 2.4, 2.3)	(2.2, 2.6, 2.1)	(2.2, 2.6, 2.1)

Table 2: Order of time convergence for (u_r, u_θ, u_ϕ) computed using the inverse Richardson extrapolation approach.

limit. Indeed, since the characteristic density $\rho_0 = 1$, the characteristic sound speed becomes $c_0 = \sqrt{\gamma p_0} \sim \sqrt{p_0}$, and the characteristic Mach number is equal to $M_0 = \frac{u_0}{c_0} \sim \frac{u_0}{\sqrt{p_0}}$. Then, non-dimensionalized pressure is given by

$$\tilde{p} = \frac{p}{p_0} = \tilde{p}_0 + M_0^2 \tilde{p}_2(r, \theta, \phi, t),$$

and the non-dimensionalized divergence

$$\frac{\nabla \cdot \mathbf{u}}{u_0} \sim M_0,$$

which is in agreement with the results from [10].

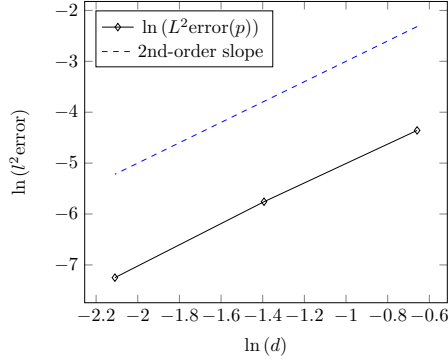
The governing equations are modified by the inclusion of source terms, computed using the manufactured solution. In all the tests presented here $p_0 = 6250$, $\gamma = \frac{c_p}{c_v} = 1.6$, $\mu = 1$, $Pr = 1$, $\boldsymbol{\omega} = \mathbf{0}$, $\mathbf{g} = \mathbf{0}$, the inner radius of the shell $R_1 = 1$, and the outer radius of the shell $R_2 = 2$. Two Picard iterations combined with the splitting error reduction are performed at each time step, initialized by $\mathbf{U}_0^{n+1} = \mathbf{U}^n$. Dirichlet boundary conditions are imposed for the velocity components at all the boundaries, and zero Neumann conditions are used for pressure and temperature (satisfied exactly by the manufactured solution). Different values of u_0 may be chosen to study the properties of the algorithm at different characteristic Mach numbers.

First, we examine space and time convergence properties at different values of M_0 . Figure 1 demonstrates the expected second order of accuracy in space for pressure (figures 1a, 1b, and 1c) and ϕ -velocity component (figures 1d, 1e, and 1f) for $M_0 = 10^{-2}$, $M_0 = 10^{-4}$, and $M_0 = 10^{-6}$ respectively. Although not shown here, velocity components in r and θ directions, and temperature exhibit similar convergence rates.

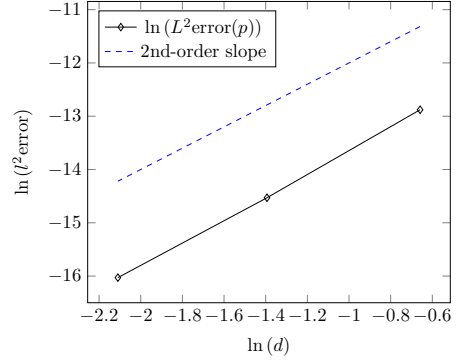
Next, we follow [11] to estimate the order of temporal accuracy using the following time convergence rate (TCR) estimate:

$$TCR(u_i, \tau) = \log_2 \left[\frac{\|u_i^\tau - u_i^{\frac{\tau}{2}}\|}{\|u_i^{\frac{\tau}{2}} - u_i^{\frac{\tau}{4}}\|} \right]$$

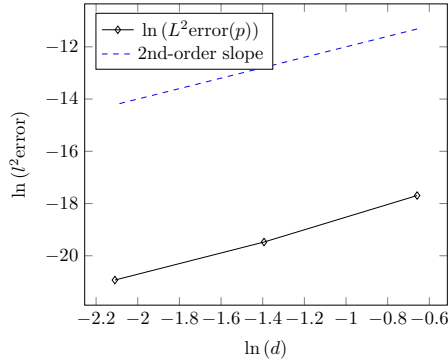
Due to the form of the TCR , spatial discretization errors cancel (i.e. the leading order truncation error is $const \cdot \tau^l$, where l is the order of accuracy in time), and $TCR \approx l$. This approach is a form of ‘‘inverse



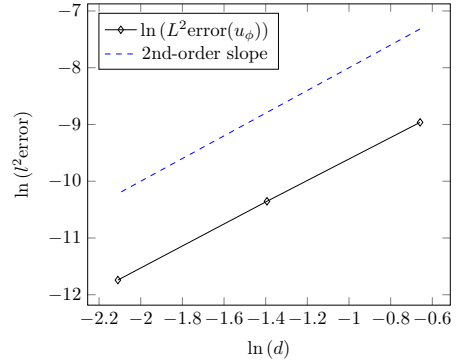
(a)



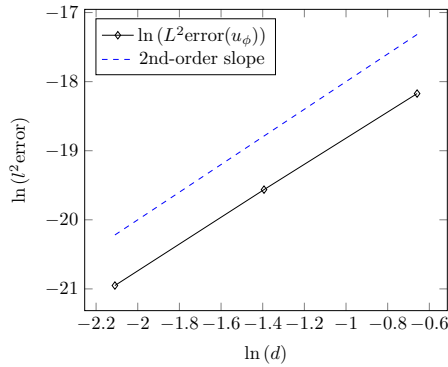
(b)



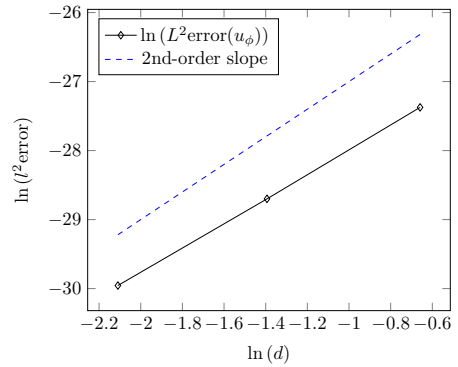
(c)



(d)



(e)



(f)

Figure 1: $\log\text{-}\log$ plots of the discrete L^2 norm of the pressure and u_ϕ errors at $t = 10^{-3}$ ($\tau = 10^{-5}$) for $M = 10^{-2}$, $M = 10^{-4}$, and $M = 10^{-6}$ manufactured solutions.

n	$M_0 = 10^{-2}$	$M_0 = 10^{-3}$	$M_0 = 10^{-4}$	$M_0 = 10^{-5}$	$M_0 = 10^{-6}$
1	$3.2 \cdot 10^{-4}$	$3.2 \cdot 10^{-6}$	$3.2 \cdot 10^{-8}$	$3.2 \cdot 10^{-10}$	$3.9 \cdot 10^{-12}$
50	$3.6 \cdot 10^{-4}$	$3.6 \cdot 10^{-6}$	$3.7 \cdot 10^{-8}$	$4.2 \cdot 10^{-10}$	$9.6 \cdot 10^{-12}$
100	$4.0 \cdot 10^{-4}$	$4.0 \cdot 10^{-6}$	$4.1 \cdot 10^{-8}$	$4.9 \cdot 10^{-10}$	$1.4 \cdot 10^{-11}$

Table 3: Maximum norm of relative pressure variations ($\Delta p = \frac{p-p_0}{p_0}$) after n time steps for different values of M_0 . $\tau = 10^{-3}$, grid diameter: 0.12.

Richardson extrapolation”, and allows temporal benchmarking of the algorithm without extreme grid refinement in 3D. The *TCR* parameters for pressure and temperature corresponding to different values of τ and M_0 are listed in Table 1, while Table 2 gives the *TCR* values for the velocity components. The results demonstrate that the temporal convergence is consistent with the theoretically expected second order.

Hence, the scheme retains its convergence properties in case of extremely low Mach numbers with no extra computational cost. Although the stability of the scheme has not been studied rigorously, based on our numerical experience the scheme is conditionally stable, as expected due to the presence of the advection terms. The stability restriction does not depend on the Mach number, at least based on the numerical tests performed for this chapter. Some dependence on the scaling of the problem, in particular on the value of p_0 , was observed.

It is well known, that in the limit to the incompressible regime, some numerical schemes can exhibit noticeable and artificial acoustic waves. Table 3 provides the maximum norm of the relative pressure fluctuations ($\Delta p = \frac{p-p_0}{p_0}$) after n time steps for different values of M_0 . Theoretically predicted order of magnitude ($\Delta p \sim \mathcal{O}(M_0^2)$) is well preserved by the scheme. The method does not introduce noticeable artificial acoustic waves ($\mathcal{O}(M_0)$ pressure fluctuations) even for extremely low values of M_0 .

# cores	1(1×1×1)	32(2×4×4)	256(4×8×8)	512(4×8×16)	1024(4×16×16)
Efficiency (one core)	–	91 %	85 %	82 %	77 %
Efficiency (one node)	–	–	93 %	90 %	85 %

Table 4: Weak Scalability test, $3375 \cdot 10^3$ grid points per core.

3.2. Weak scalability.

Next, we demonstrate the parallel performance of the method by providing weak scalability results. We consider $3375 \cdot 10^3$ grid points per core and measure the efficiency on 32 cores (1 computational node), 256 cores (8 nodes), 512 cores (16 nodes), and 1024 cores (32 nodes). The efficiency results are given in Table 4. The efficiency is given relative to 1 core and relative to 1 node since the drop in efficiency from 1 to 32 cores is likely caused by the need to share the memory bandwidth and cache with a smaller number of cores within the computational node, rather than scaling properties of the method (see e.g. [12], p. 152). The weak scaling test demonstrates excellent parallel performance.

The scaling tests are performed using the Compute Canada Graham cluster (see <https://www.computecanada.ca/>) of 2.1GHz Intel *E5 – 2683 v4* CPU cores, 32 cores per node, and each node connected via a 100 Gb/s network. The results were calculated using the wall clock time taken to simulate 10 time steps with two Picard iterations each. These computations were performed three times for each configuration, and the average wall clock time was used to compute the efficiency.

4. Conclusion.

The numerical experiments presented above demonstrate the effectiveness of implicit methods based on the direction splitting approach for modelling compressible flows in spherical shells in nearly incompressible and weakly compressible regimes. The proposed algorithm retains theoretically expected convergence rates and remains stable for extremely small values of the characteristic Mach number (at least as low as $M_0 = 10^{-6}$). The staggered spatial discretization on the MAC stencil, commonly used in numerical methods for incompressible Navier-Stokes equations, was found to be convenient for the discretization of the compressible Navier-Stokes equations written in the non-conservative form in terms of the primitive variables. This approach helped to avoid the high-frequency oscillations without any artificial stabilization terms. Nonlinear Picard iterations with the splitting error reduction were also implemented to allow one to obtain a solution of the fully nonlinear system of equations.

These results, alongside excellent parallel performance, prove the viability of the direction splitting approach in large-scale high-resolution high-performance simulations of atmospheric and oceanic flows. Possibilities for future studies and developments include research of monotonicity preserving properties of the scheme to evaluate the need for stabilization terms for flows under extreme conditions, such as high Reynolds numbers. The influence of the linearization error on the monotonicity and stability is worth investigating as well. The computational domain should be modified to represent realistic topography, and the adaptive mesh refinement is likely to be necessary for practical applications in oceanography and atmospheric sciences.

Acknowledgments

The authors would like to acknowledge the support, under a Discovery Grant, of the National Science and Engineering Research Council of Canada (NSERC).

This research was enabled in part by support provided by Compute Canada (www.computecanada.ca).

Appendix A. Compressible Navier-Stokes equations for dry atmosphere in primitive variables.

The dry dynamics of Earth's atmosphere can be modeled by the compressible Navier-Stokes equations written in the conservative form in terms of density ρ [kg/m^3], velocity \mathbf{u} [$m/s, m/s, m/s$] – Cartesian or [$m/s, 1/s, 1/s$] – spherical, and the total energy per unit volume E [J/m^3] (see [1]):

$$\frac{\partial \rho}{\partial t} + \nabla \cdot (\rho \mathbf{u}) = 0 \quad (4.1)$$

$$\frac{\partial \rho \mathbf{u}}{\partial t} + \nabla \cdot (\rho \mathbf{u} \otimes \mathbf{u}) + \nabla p + 2\rho(\boldsymbol{\omega} \times \mathbf{u}) + \rho \mathbf{g} - \nabla \cdot \hat{\boldsymbol{\sigma}} = 0 \quad (4.2)$$

$$\frac{\partial E}{\partial t} + \nabla \cdot ((E + p)\mathbf{u}) - \nabla \cdot \left(\frac{\mu c_p}{Pr} \nabla T + \mathbf{u} \cdot \hat{\boldsymbol{\sigma}} \right) = 0 \quad (4.3)$$

where $\boldsymbol{\omega}$ [1/s, 1/s, 1/s] is the rotational velocity of the Earth, $\hat{\boldsymbol{\sigma}}$ is the viscous stress tensor given by

$$\hat{\boldsymbol{\sigma}} = \mu \left[(\nabla \mathbf{u} + (\nabla \mathbf{u})^T) - \frac{2}{3} (\nabla \cdot \mathbf{u}) \hat{I} \right],$$

\mathbf{g} [$m/s^2, m/s^2, m/s^2$] – Cartesian or [$m/s^2, 1/s^2, 1/s^2$] – spherical, is the sum of the true gravity and the centrifugal force, c_p [$J/(K \cdot kg)$], c_v [$J/(K \cdot kg)$], μ [$kg/(s \cdot m)$], Pr, $\gamma = \frac{c_p}{c_v}$, π_∞ [Pa] are constant for each material. The total energy E is the sum of the internal energy ($e = c_v T + \frac{\pi_\infty}{\rho}$), kinetic energy, and gravitational potential energy:

$$E = \rho e + \frac{1}{2} \rho \mathbf{u} \cdot \mathbf{u} + \rho g r \quad (4.4)$$

where r [m] is the radial distance from the center of the Earth. The viscous stress tensor for a Newtonian fluid is given by

$$\hat{\boldsymbol{\sigma}} = \mu \left[(\nabla \mathbf{u} + (\nabla \mathbf{u})^T) - \frac{2}{3} (\nabla \cdot \mathbf{u}) \hat{I} \right]. \quad (4.5)$$

Pressure is given through the Stiffened Gas Equation of State:

$$p = (\gamma - 1) \rho e - \gamma \pi_\infty. \quad (4.6)$$

The goal of this appendix is to re-write equations (4.1)-(4.3) in the non-conservative form in terms of the primitive variables p [Pa], \mathbf{u} [$m/s, m/s, m/s$] – Cartesian or [$m/s, 1/s, 1/s$] – spherical, and T [K]. Then, density will be given by the following equation of state (equivalent to 4.6):

$$\rho = \frac{p + \pi_\infty}{c_v (\gamma - 1) T}. \quad (4.7)$$

First, we work with the momentum conservation equation (4.2). Using the chain rule:

$$\frac{\partial \rho \mathbf{u}}{\partial t} = \rho \frac{\partial \mathbf{u}}{\partial t} + \mathbf{u} \frac{\partial \rho}{\partial t},$$

$$\nabla \cdot (\rho \mathbf{u} \otimes \mathbf{u}) = \rho \mathbf{u} \cdot \nabla \mathbf{u} + \nabla \cdot (\rho \mathbf{u}) \mathbf{u}.$$

Hence, (4.2) becomes

$$\rho \left[\frac{\partial \mathbf{u}}{\partial t} + \mathbf{u} \cdot \nabla \mathbf{u} + \frac{1}{\rho} \nabla p - \frac{1}{\rho} \nabla \cdot \hat{\boldsymbol{\sigma}} + \mathbf{g} + 2(\mathbf{u} \times \boldsymbol{\omega}) \right] + \mathbf{u} \left[\frac{\partial \rho}{\partial t} + \nabla \cdot (\rho \mathbf{u}) \right] = 0$$

Since the expression in the second brackets is zero due to the mass conservation (4.1), the momentum conservation can be re-written in the non-conservative form as:

$$\frac{\partial \mathbf{u}}{\partial t} + \mathbf{u} \cdot \nabla \mathbf{u} + \frac{1}{\rho} \nabla p - \frac{1}{\rho} \nabla \cdot \hat{\boldsymbol{\sigma}} + \mathbf{g} + 2(\mathbf{u} \times \boldsymbol{\omega}) = 0. \quad (4.8)$$

Next, we look at the energy conservation equation (4.3). For convenience, we denote

$$Q = -\nabla \cdot \left(\frac{\mu c_p}{Pr} \nabla T + \mathbf{u} \cdot \hat{\boldsymbol{\sigma}} \right),$$

and then (4.3) can be re-written as

$$\frac{\partial E}{\partial t} + \nabla \cdot ((E + p) \mathbf{u}) + Q = 0.$$

We can express the total energy as:

$$E = \rho c_V T + \pi_\infty + \frac{\rho \mathbf{u} \cdot \mathbf{u}}{2} + \rho gr = \frac{p + \pi_\infty}{\gamma - 1} + \pi_\infty + \frac{\rho \mathbf{u} \cdot \mathbf{u}}{2} + \rho gr = \frac{p}{\gamma - 1} + \frac{\gamma \pi_\infty}{\gamma - 1} + \frac{\rho \mathbf{u} \cdot \mathbf{u}}{2} + \rho gr.$$

Substituting the last expression for energy into (4.3) gives:

$$\left[\partial_t \left(\frac{p}{\gamma - 1} \right) + \nabla \cdot \left(\frac{p}{\gamma - 1} \mathbf{u} \right) + \nabla \cdot (p \mathbf{u}) \right] + \left[\partial_t \left(\frac{\pi_\infty \gamma}{\gamma - 1} \right) + \nabla \cdot \left(\frac{\pi_\infty \gamma}{\gamma - 1} \mathbf{u} \right) \right] + \left[\partial_t \left(\frac{\rho \mathbf{u} \cdot \mathbf{u}}{2} \right) + \nabla \cdot \left(\frac{\rho \mathbf{u} \cdot \mathbf{u}}{2} \mathbf{u} \right) \right] + [\partial_t(\rho gr) + \nabla \cdot (\rho gr \mathbf{u})] + Q = 0$$

Considering all the expressions in brackets above one by one, and using (4.1), one obtains

$$\begin{aligned} \partial_t(\rho gr) + \nabla \cdot (\rho gr \mathbf{u}) &= g(r \partial_t \rho + r \rho \nabla \cdot \mathbf{u} + r \nabla \rho \cdot \mathbf{u} + \rho \nabla r \cdot \mathbf{u}) = \\ &= g(r(\partial_t \rho + \nabla \cdot (\rho \mathbf{u})) + \rho \nabla r \cdot \mathbf{u}) = gr \nabla r \cdot \mathbf{u} = g \rho u_r, \end{aligned}$$

$$\begin{aligned} \frac{1}{2}(\partial_t(\rho \mathbf{u} \cdot \mathbf{u}) + \nabla \cdot ((\rho \mathbf{u} \cdot \mathbf{u}) \mathbf{u})) &= \frac{1}{2}((\mathbf{u} \cdot \mathbf{u}) \partial_t \rho + \rho \partial_t(\mathbf{u} \cdot \mathbf{u}) + (\rho \mathbf{u} \cdot \mathbf{u}) \nabla \cdot \mathbf{u} + \mathbf{u} \cdot \nabla(\rho \mathbf{u} \cdot \mathbf{u})) = \\ &= \frac{\mathbf{u} \cdot \mathbf{u}}{2} [\partial_t \rho + \rho \nabla \cdot \mathbf{u} + \mathbf{u} \cdot \nabla \rho] + \frac{\rho}{2} [\partial_t(\mathbf{u} \cdot \mathbf{u}) + \mathbf{u} \cdot \nabla(\mathbf{u} \cdot \mathbf{u})] = \rho \mathbf{u} \cdot [\partial_t \mathbf{u} + (\mathbf{u} \cdot \nabla) \mathbf{u}]. \end{aligned}$$

Then, using (4.8):

$$\begin{aligned} \frac{1}{2}(\partial_t(\rho \mathbf{u} \cdot \mathbf{u}) + \nabla \cdot ((\rho \mathbf{u} \cdot \mathbf{u}) \mathbf{u})) &= \rho \mathbf{u} \cdot \left[-\frac{1}{\rho} \nabla p - \mathbf{g} - 2\boldsymbol{\omega} \times \mathbf{u} + \frac{1}{\rho} \nabla \cdot \hat{\boldsymbol{\sigma}} \right] = \\ &= -\mathbf{u} \cdot \nabla p - \rho \mathbf{u} \cdot \mathbf{g} - 2\rho \mathbf{u} \cdot (\boldsymbol{\omega} \times \mathbf{u}) + \mathbf{u} \cdot (\nabla \cdot \hat{\boldsymbol{\sigma}}). \end{aligned}$$

Since $\mathbf{u} \cdot \mathbf{g} = g u_r$ and \mathbf{u} is perpendicular to $\boldsymbol{\omega} \times \mathbf{u}$, (4.3) becomes:

$$\begin{aligned} \partial_t \left(\frac{p}{\gamma - 1} \right) + \nabla \cdot \left(\frac{p}{\gamma - 1} \mathbf{u} \right) + \nabla \cdot (p \mathbf{u}) + \partial_t \left(\frac{\pi_\infty \gamma}{\gamma - 1} \right) + \\ \nabla \cdot \left(\frac{\pi_\infty \gamma}{\gamma - 1} \mathbf{u} \right) - \mathbf{u} \cdot \nabla p + \mathbf{u} \cdot (\nabla \cdot \hat{\boldsymbol{\sigma}}) + Q = 0 \end{aligned} \quad (4.9)$$

Let $V = \mathbf{u} \cdot (\nabla \cdot \hat{\boldsymbol{\sigma}}) + Q$. Applying the chain rule to the terms in (4.9) and re-arranging them we get:

$$\begin{aligned} \frac{1}{\gamma - 1} \left[\frac{\partial p}{\partial t} + p \nabla \cdot \mathbf{u} + (\gamma - 1)p \nabla \cdot \mathbf{u} + \mathbf{u} \cdot \nabla p + \pi_\infty \gamma \nabla \cdot \mathbf{u} \right] + V + \\ p \left[\partial_t \left(\frac{1}{\gamma - 1} \right) + \mathbf{u} \cdot \nabla \left(\frac{1}{\gamma - 1} \right) \right] + \left[\partial_t \left(\frac{\pi_\infty \gamma}{\gamma - 1} \right) + \mathbf{u} \cdot \nabla \left(\frac{\pi_\infty \gamma}{\gamma - 1} \right) \right] = 0. \end{aligned}$$

Since equations

$$\partial_t \left(\frac{1}{\gamma - 1} \right) + \mathbf{u} \cdot \nabla \left(\frac{1}{\gamma - 1} \right) = 0$$

and

$$\partial_t \left(\frac{\pi_\infty \gamma}{\gamma - 1} \right) + \mathbf{u} \cdot \nabla \left(\frac{\pi_\infty \gamma}{\gamma - 1} \right) = 0$$

represent the advection of a material interface and thus have to be satisfied, (4.3) can be written as:

$$\frac{\partial p}{\partial t} + \mathbf{u} \cdot \nabla p + \gamma(p + \pi_\infty) \nabla \cdot \mathbf{u} + (\gamma - 1)V = 0. \quad (4.10)$$

Finally, we re-write (4.1) as:

$$\frac{\partial \rho}{\partial t} + \mathbf{u} \cdot \nabla \rho + \rho \nabla \cdot \mathbf{u} = 0.$$

Since

$$\rho = \frac{p}{c_V(\gamma-1)T} + \frac{\pi_\infty}{c_V(\gamma-1)T},$$

we compute:

$$\begin{aligned} \frac{\partial \rho}{\partial t} &= \frac{1}{c_V(\gamma-1)T} \frac{\partial p}{\partial t} - \frac{p}{c_V(\gamma-1)T^2} \frac{\partial T}{\partial t} + \frac{p}{T} \partial_t \left(\frac{1}{c_V(\gamma-1)} \right) \\ &\quad + \frac{1}{T} \partial_t \left(\frac{\pi_\infty}{c_V(\gamma-1)} \right) - \frac{\pi_\infty}{c_V(\gamma-1)T^2} \frac{\partial T}{\partial t}, \\ \nabla \rho &= \frac{1}{c_V(\gamma-1)T} \nabla p - \frac{p}{c_V(\gamma-1)T^2} \nabla T + \frac{p}{T} \nabla \left(\frac{1}{c_V(\gamma-1)} \right) \\ &\quad + \frac{1}{T} \nabla \left(\frac{\pi_\infty}{c_V(\gamma-1)} \right) - \frac{\pi_\infty}{c_V(\gamma-1)T^2} \nabla T, \end{aligned}$$

and the mass conservation equation (4.1) becomes:

$$\begin{aligned} &\frac{1}{c_V(\gamma-1)T} \left[\frac{\partial p}{\partial t} + \mathbf{u} \cdot \nabla p \right] - \frac{p + \pi_\infty}{c_V(\gamma-1)T^2} \left[\frac{\partial T}{\partial t} + \mathbf{u} \cdot \nabla T \right] + \frac{p + \pi_\infty}{c_V(\gamma-1)T} \nabla \cdot \mathbf{u} + \\ &\frac{p}{T} \left[\frac{\partial}{\partial t} \left(\frac{1}{c_V(\gamma-1)} \right) + \mathbf{u} \cdot \nabla \left(\frac{1}{c_V(\gamma-1)} \right) \right] + \frac{1}{T} \left[\frac{\partial}{\partial t} \left(\frac{\pi_\infty}{c_V(\gamma-1)} \right) + \mathbf{u} \cdot \nabla \left(\frac{\pi_\infty}{c_V(\gamma-1)} \right) \right] = 0 \end{aligned}$$

Since

$$\frac{\partial}{\partial t} \left(\frac{1}{c_V(\gamma-1)} \right) + \mathbf{u} \cdot \nabla \left(\frac{1}{c_V(\gamma-1)} \right) = 0$$

and

$$\frac{\partial}{\partial t} \left(\frac{\pi_\infty}{c_V(\gamma-1)} \right) + \mathbf{u} \cdot \nabla \left(\frac{\pi_\infty}{c_V(\gamma-1)} \right) = 0$$

represent the advection of a material interface and thus have to be satisfied, and $\frac{\partial p}{\partial t} + \mathbf{u} \cdot \nabla p$ can be expressed from (4.10), the mass conservation can be written in the non-conservative form as:

$$\frac{\partial T}{\partial t} + \mathbf{u} \cdot \nabla T + (\gamma-1)T \nabla \cdot \mathbf{u} + \frac{(\gamma-1)T}{p + \pi_\infty} V = 0. \quad (4.11)$$

Recall that

$$V = -\nabla \cdot \left(\frac{\mu c_p}{Pr} \nabla T \right) - \nabla \cdot (\mathbf{u} \cdot \hat{\boldsymbol{\sigma}}) + \mathbf{u} \cdot (\nabla \cdot \hat{\boldsymbol{\sigma}}).$$

Using the symmetry of the stress tensor we obtain:

$$\begin{aligned} \nabla \cdot (\mathbf{u} \cdot \hat{\boldsymbol{\sigma}}) - \mathbf{u} \cdot (\nabla \cdot \hat{\boldsymbol{\sigma}}) &= \partial_i (u_j \sigma_{ij}) - u_j \partial_i \sigma_{ji} = (\partial_i u_j) \sigma_{ij} + u_j \partial_i \sigma_{ij} - u_j \partial_i \sigma_{ji} = \\ &(\partial_i u_j) \sigma_{ij} + u_j \partial_i \sigma_{ij} - u_j \partial_i \sigma_{ij} = (\partial_i u_j) \sigma_{ij} = \nabla \mathbf{u} : \hat{\boldsymbol{\sigma}}, \end{aligned}$$

and thus V becomes

$$V = -\nabla \cdot \left(\frac{\mu c_p}{Pr} \nabla T \right) - \nabla \mathbf{u} : \hat{\boldsymbol{\sigma}}. \quad (4.12)$$

Substituting (4.12) into (4.10) and (4.11), we finally write the system (4.1)-(4.3) in the non-conservative form in terms of the primitive variables (p, \mathbf{u}, T) :

$$\begin{aligned} \frac{\partial T}{\partial t} + \mathbf{u} \cdot \nabla T + (\gamma - 1)T \nabla \cdot \mathbf{u} - \frac{(\gamma - 1)T}{p + \pi_\infty} \nabla \cdot \left(\frac{\mu c_p}{Pr} \nabla T \right) \\ - \frac{(\gamma - 1)T}{p + \pi_\infty} \nabla \mathbf{u} : \hat{\boldsymbol{\sigma}} = 0, \end{aligned} \quad (4.13)$$

$$\frac{\partial \mathbf{u}}{\partial t} + \mathbf{u} \cdot \nabla \mathbf{u} + \frac{1}{\rho} \nabla p - \frac{1}{\rho} \nabla \cdot \hat{\boldsymbol{\sigma}} + \mathbf{g} + 2(\mathbf{u} \times \boldsymbol{\omega}) = 0, \quad (4.14)$$

$$\begin{aligned} \frac{\partial p}{\partial t} + \mathbf{u} \cdot \nabla p + \gamma(p + \pi_\infty) \nabla \cdot \mathbf{u} - (\gamma - 1) \nabla \cdot \left(\frac{\mu c_p}{Pr} \nabla T \right) \\ - (\gamma - 1) \nabla \mathbf{u} : \hat{\boldsymbol{\sigma}} = 0, \end{aligned} \quad (4.15)$$

where

$$\rho = \frac{p + \pi_\infty}{c_V(\gamma - 1)T}. \quad (4.16)$$

Appendix B. Governing equations in spherical coordinates and definition of operators.

Here we aim at rewriting the following system of PDEs in spherical coordinates:

$$\begin{aligned} \frac{\partial T}{\partial t} + \mathbf{u} \cdot \nabla T + (\gamma - 1)T \nabla \cdot \mathbf{u} - \frac{(\gamma - 1)T}{p + \pi_\infty} \nabla \cdot \left(\frac{\mu c_p}{Pr} \nabla T \right) \\ - \frac{(\gamma - 1)T}{p + \pi_\infty} \nabla \mathbf{u} : \hat{\boldsymbol{\sigma}} = 0, \end{aligned} \quad (4.17)$$

$$\frac{\partial \mathbf{u}}{\partial t} + \mathbf{u} \cdot \nabla \mathbf{u} + \frac{1}{\rho} \nabla p - \frac{1}{\rho} \nabla \cdot \hat{\boldsymbol{\sigma}} + \mathbf{g} + 2(\mathbf{u} \times \boldsymbol{\omega}) = 0, \quad (4.18)$$

$$\begin{aligned} \frac{\partial p}{\partial t} + \mathbf{u} \cdot \nabla p + \gamma(p + \pi_\infty) \nabla \cdot \mathbf{u} - (\gamma - 1) \nabla \cdot \left(\frac{\mu c_p}{Pr} \nabla T \right) \\ - (\gamma - 1) \nabla \mathbf{u} : \hat{\boldsymbol{\sigma}} = 0. \end{aligned} \quad (4.19)$$

where

$$\rho = \frac{p + \pi_\infty}{c_V(\gamma - 1)T}. \quad (4.20)$$

First, we provide expressions for all the spherical differential operators used in (4.17)-(4.19). Recall that the spherical transformation is given by:

$$\begin{cases} x &= r \sin \theta \cos \phi \\ y &= r \sin \theta \sin \phi \\ z &= r \cos \theta, \end{cases}$$

where $r \in [R_1, R_2]$, $\theta \in [0, \pi]$, $\phi \in [0, 2\pi]$. We also denote by \mathbf{e}_r , \mathbf{e}_θ , and \mathbf{e}_ϕ the corresponding unit vectors in spherical coordinates, and the spherical unit tensors by $\mathbf{e}_{z\mathbf{l}}$, where $z, l = r, \theta, \text{ or } \phi$. Then,

$$\begin{aligned}
\nabla \cdot \mathbf{u} &= \frac{1}{r^2} \frac{\partial (r^2 u_r)}{\partial r} + \frac{1}{r \sin \theta} \frac{\partial (u_\theta \sin \theta)}{\partial \theta} + \frac{1}{r \sin \theta} \frac{\partial (u_\phi)}{\partial \phi} \\
\nabla f &= \frac{\partial f}{\partial r} \mathbf{e}_r + \frac{1}{r} \frac{\partial f}{\partial \theta} \mathbf{e}_\theta + \frac{1}{r \sin \theta} \frac{\partial f}{\partial \phi} \mathbf{e}_\phi \\
\nabla^2 f &= \frac{1}{r^2} \frac{\partial}{\partial r} \left(r^2 \frac{\partial f}{\partial r} \right) + \frac{1}{r^2 \sin \theta} \frac{\partial}{\partial \theta} \left(\sin \theta \frac{\partial f}{\partial \theta} \right) + \frac{1}{r^2 \sin^2 \theta} \frac{\partial^2 f}{\partial \phi^2} \\
\nabla \mathbf{u} = \hat{G} &= \frac{\partial u_r}{\partial r} \mathbf{e}_{rr} + \frac{\partial u_\theta}{\partial r} \mathbf{e}_{r\theta} + \frac{\partial u_\phi}{\partial r} \mathbf{e}_{r\phi} + \\
&\quad \left(\frac{1}{r} \frac{\partial u_r}{\partial \theta} - \frac{u_\theta}{r} \right) \mathbf{e}_{\theta r} + \left(\frac{1}{r} \frac{\partial u_\theta}{\partial \theta} + \frac{u_r}{r} \right) \mathbf{e}_{\theta\theta} + \left(\frac{1}{r} \frac{\partial u_\phi}{\partial \theta} \right) \mathbf{e}_{\theta\phi} + \\
&\quad \left(\frac{1}{r \sin \theta} \frac{\partial u_r}{\partial \phi} - \frac{u_\phi}{r} \right) \mathbf{e}_{\phi r} + \left(\frac{1}{r \sin \theta} \frac{\partial u_\theta}{\partial \phi} - \frac{u_\phi}{r \tan \theta} \right) \mathbf{e}_{\phi\theta} + \\
&\quad \left(\frac{1}{r \sin \theta} \frac{\partial u_\phi}{\partial \phi} + \frac{u_\theta}{r \tan \theta} + \frac{u_r}{r} \right) \mathbf{e}_{\phi\phi} \\
\nabla^2 \mathbf{u} &= \left(\nabla^2 u_r - \frac{2u_r}{r^2} - \frac{2}{r^2 \sin \theta} \frac{\partial (u_\theta \sin \theta)}{\partial \theta} - \frac{2}{r^2 \sin \theta} \frac{\partial u_\phi}{\partial \phi} \right) \mathbf{e}_r + \\
&\quad \left(\nabla^2 u_\theta - \frac{u_\theta}{r^2 \sin^2 \theta} + \frac{2}{r^2} \frac{\partial u_r}{\partial \theta} - \frac{2 \cos \theta}{r^2 \sin^2 \theta} \frac{\partial u_\phi}{\partial \phi} \right) \mathbf{e}_\theta + \\
&\quad \left(\nabla^2 u_\phi - \frac{u_\phi}{r^2 \sin^2 \theta} + \frac{2}{r^2 \sin \theta} \frac{\partial u_r}{\partial \phi} + \frac{2 \cos \theta}{r^2 \sin^2 \theta} \frac{\partial u_\theta}{\partial \phi} \right) \mathbf{e}_\phi \\
\nabla \cdot (\mu \nabla \mathbf{u}) &= \left(\nabla \cdot (\mu \nabla u_r) - \frac{2\mu u_r}{r^2} \right) \mathbf{e}_r + \\
&\quad \left(-\frac{\mu}{r^2 \sin \theta} \frac{\partial (u_\theta \sin \theta)}{\partial \theta} - \frac{\mu}{r^2 \sin \theta} \frac{\partial u_\phi}{\partial \phi} - \frac{1}{r^2 \sin \theta} \frac{\partial (\mu u_\theta \sin \theta)}{\partial \theta} - \frac{1}{r^2 \sin \theta} \frac{\partial (\mu u_\phi)}{\partial \phi} \right) \mathbf{e}_r + \\
&\quad \left(\nabla \cdot (\mu \nabla u_\theta) - \frac{\mu u_\theta}{r^2 \sin^2 \theta} \right) \mathbf{e}_\theta + \\
&\quad \left(\frac{\mu}{r^2} \frac{\partial u_r}{\partial \theta} - \frac{\mu \cos \theta}{r^2 \sin^2 \theta} \frac{\partial u_\phi}{\partial \phi} + \frac{1}{r^2} \frac{\partial (\mu u_r)}{\partial \theta} - \frac{\cos \theta}{r^2 \sin^2 \theta} \frac{\partial (\mu u_\phi)}{\partial \phi} \right) \mathbf{e}_\theta + \\
&\quad \left(\nabla \cdot (\mu \nabla u_\phi) - \frac{\mu u_\phi}{r^2 \sin^2 \theta} \right) \mathbf{e}_\phi + \\
&\quad \left(\frac{\mu}{r^2 \sin \theta} \frac{\partial u_r}{\partial \phi} + \frac{\mu \cos \theta}{r^2 \sin^2 \theta} \frac{\partial u_\theta}{\partial \phi} + \frac{1}{r^2 \sin \theta} \frac{\partial (\mu u_r)}{\partial \phi} + \frac{\cos \theta}{r^2 \sin^2 \theta} \frac{\partial (\mu u_\theta)}{\partial \phi} \right) \mathbf{e}_\phi \\
\nabla \nabla \cdot \mathbf{u} &= \left(\frac{\partial}{\partial r} \left[\frac{1}{r^2} \frac{\partial (r^2 u_r)}{\partial r} \right] + \frac{\partial}{\partial r} \left[\frac{1}{r \sin \theta} \frac{\partial (u_\theta \sin \theta)}{\partial \theta} \right] + \frac{\partial}{\partial r} \left[\frac{1}{r \sin \theta} \frac{\partial u_\phi}{\partial \phi} \right] \right) \mathbf{e}_r + \\
&\quad \left(\frac{1}{r^3} \frac{\partial^2 (r^2 u_r)}{\partial \theta \partial r} + \frac{1}{r^2} \frac{\partial}{\partial \theta} \left[\frac{1}{\sin \theta} \frac{\partial (u_\theta \sin \theta)}{\partial \theta} \right] + \frac{1}{r^2} \frac{\partial}{\partial \theta} \left[\frac{1}{\sin \theta} \frac{\partial u_\phi}{\partial \phi} \right] \right) \mathbf{e}_\theta + \\
&\quad \left(\frac{1}{r^3 \sin \theta} \frac{\partial^2 (r^2 u_r)}{\partial \phi \partial r} + \frac{1}{r^2 \sin^2 \theta} \frac{\partial^2 (u_\theta \sin \theta)}{\partial \phi \partial \theta} + \frac{1}{r^2 \sin^2 \theta} \frac{\partial^2 u_\phi}{\partial \phi^2} \right) \mathbf{e}_\phi
\end{aligned}$$

Notice that

$$\nabla \cdot \hat{\sigma} = \nabla \cdot (\mu \nabla \mathbf{u}) + \nabla \cdot \left(\frac{\mu}{3} \nabla \cdot \mathbf{u} \right).$$

And finally, the stress tensor is equal to

$$\begin{aligned}
\hat{\boldsymbol{\sigma}} = & \mu \left[2 \frac{\partial u_r}{\partial r} - \frac{2}{3} \left(\frac{1}{r^2} \frac{\partial}{\partial r} (r^2 u_r) + \frac{1}{r \sin \theta} \frac{\partial}{\partial \theta} (\sin \theta u_\theta) + \frac{1}{r \sin \theta} \frac{\partial u_\phi}{\partial \phi} \right) \right] \mathbf{e}_{rr} \\
& + \mu \left[\frac{\partial u_\theta}{\partial r} + \frac{1}{r} \frac{\partial u_r}{\partial \theta} - \frac{u_\theta}{r} \right] \mathbf{e}_{r\theta} \\
& + \mu \left[\frac{\partial u_\phi}{\partial r} + \frac{1}{r \sin \theta} \frac{\partial u_r}{\partial \phi} - \frac{u_\phi}{r} \right] \mathbf{e}_{r\phi} \\
& + \mu \left[\frac{\partial u_\theta}{\partial r} + \frac{1}{r} \frac{\partial u_r}{\partial \theta} - \frac{u_\theta}{r} \right] \mathbf{e}_{\theta r} \\
& + \mu \left[\frac{2}{r} \frac{\partial u_\theta}{\partial \theta} + \frac{2u_r}{r} - \frac{2}{3} \left(\frac{1}{r^2} \frac{\partial}{\partial r} (r^2 u_r) + \frac{1}{r \sin \theta} \frac{\partial}{\partial \theta} (\sin \theta u_\theta) + \frac{1}{r \sin \theta} \frac{\partial u_\phi}{\partial \phi} \right) \right] \mathbf{e}_{\theta\theta} \\
& + \mu \left[\frac{1}{r} \frac{\partial u_\phi}{\partial \theta} + \frac{1}{r \sin \theta} \frac{\partial u_\theta}{\partial \phi} - \frac{u_\phi}{r \tan \theta} \right] \mathbf{e}_{\theta\phi} \\
& + \mu \left[\frac{\partial u_\phi}{\partial r} + \frac{1}{r \sin \theta} \frac{\partial u_r}{\partial \phi} - \frac{u_\phi}{r} \right] \mathbf{e}_{\phi r} \\
& + \mu \left[\frac{1}{r} \frac{\partial u_\phi}{\partial \theta} + \frac{1}{r \sin \theta} \frac{\partial u_\theta}{\partial \phi} - \frac{u_\phi}{r \tan \theta} \right] \mathbf{e}_{\phi\theta} \\
& + \mu \left[\frac{2}{r \sin \theta} \frac{\partial u_\phi}{\partial \phi} + \frac{2u_\theta}{r \tan \theta} + \frac{2u_r}{r} - \frac{2}{3} \left(\frac{1}{r^2} \frac{\partial}{\partial r} (r^2 u_r) + \frac{1}{r \sin \theta} \frac{\partial}{\partial \theta} (\sin \theta u_\theta) + \frac{1}{r \sin \theta} \frac{\partial u_\phi}{\partial \phi} \right) \right] \mathbf{e}_{\phi\phi}
\end{aligned}$$

To simplify the notations, we define the following operators:

$$\mathbf{A}_1(\mathbf{u})f = \mathbf{u} \cdot \nabla f \quad (4.21)$$

$$\mathbf{A}_2(p, \mathbf{u})\mathbf{v} = \gamma (p + \pi_\infty) \nabla \cdot \mathbf{v} - (\gamma - 1) \nabla \mathbf{u} : \hat{\boldsymbol{\sigma}}(\mathbf{v}) \quad (4.22)$$

$$\mathbf{A}_3 f = -(\gamma - 1) \nabla \cdot \left(\frac{\mu c_p}{Pr} \nabla f \right) \quad (4.23)$$

$$\mathbf{B}_1(\rho)f = \frac{1}{\rho} \nabla f \quad (4.24)$$

$$\mathbf{B}_2(\rho, \mathbf{u})\mathbf{v} = \mathbf{u} \cdot \nabla \mathbf{v} + 2(\boldsymbol{\omega} \times \mathbf{v}) - \frac{1}{\rho} \left(\nabla \cdot (\mu \nabla \mathbf{v}) + \nabla \left(\frac{\mu}{3} \nabla \cdot \mathbf{v} \right) \right) \quad (4.25)$$

$$\mathbf{C}_2(T, p, \mathbf{u})\mathbf{v} = (\gamma - 1) T \nabla \cdot \mathbf{v} - \frac{(\gamma - 1) T}{p + \pi_\infty} \nabla \mathbf{u} : \hat{\boldsymbol{\sigma}}(\mathbf{v}) \quad (4.26)$$

$$\mathbf{C}_3(T, p, \mathbf{u})f = \mathbf{u} \cdot \nabla f - \frac{(\gamma - 1) T}{p + \pi_\infty} \nabla \cdot \left(\frac{\mu c_p}{Pr} \nabla f \right) \quad (4.27)$$

Thus, the system (4.17)-(4.19) can be written as

$$\frac{\partial p}{\partial t} + \mathbf{A}_1(\mathbf{u})p + \mathbf{A}_2(p, \mathbf{u})\mathbf{u} + \mathbf{A}_3 T = 0, \quad (4.28)$$

$$\frac{\partial \mathbf{u}}{\partial t} + \mathbf{B}_1(\rho)p + \mathbf{B}_2(\rho, \mathbf{u})\mathbf{u} + \mathbf{g} = 0, \quad (4.29)$$

$$\frac{\partial T}{\partial t} + \mathbf{C}_2(T, p, \mathbf{u})\mathbf{u} + \mathbf{C}_3(T, p, \mathbf{u})T = 0. \quad (4.30)$$

The operators (4.21) - (4.27) can be splitted direction-wise as following (note that the operators with the upper subindex M include mixed derivatives, derivatives in staggered directions, and other terms that cannot be naturally incorporated into the direction splitting approach implicitly):

$$\mathbf{A}_1 f = \mathbf{A}_1^r f + \mathbf{A}_1^\theta f + \mathbf{A}_1^\phi f = u_r \frac{\partial f}{\partial r} + \frac{u_\theta}{r} \frac{\partial f}{\partial \theta} + \frac{u_\phi}{r \sin \theta} \frac{\partial f}{\partial \phi}$$

$$\mathbf{A}_2 \mathbf{v} = \mathbf{A}_2^r \mathbf{v} + \mathbf{A}_2^\theta \mathbf{v} + \mathbf{A}_2^\phi \mathbf{v} + \mathbf{A}_2^M \mathbf{v}$$

$$\begin{aligned} \mathbf{A}_2^r \mathbf{v} &= \left(\gamma(p + \pi_\infty) + \frac{2\mu(\gamma-1)}{3} (\hat{G}_{rr} + \hat{G}_{\theta\theta} + \hat{G}_{\phi\phi}) \right) \frac{1}{r^2} \frac{\partial (r^2 v_r)}{\partial r} - \\ &\quad 2\mu(\gamma-1) \hat{G}_{rr} \frac{\partial v_r}{\partial r} - \mu(\gamma-1) \left(2\hat{G}_{\theta\theta} + 2\hat{G}_{\phi\phi} \right) \frac{v_r}{r} \\ \mathbf{A}_2^\theta \mathbf{v} &= \left(\gamma(p + \pi_\infty) + \frac{2\mu(\gamma-1)}{3} (\hat{G}_{rr} + \hat{G}_{\theta\theta} + \hat{G}_{\phi\phi}) \right) \frac{1}{r \sin \theta} \frac{\partial (\sin \theta v_\theta)}{\partial \theta} - \\ &\quad 2\mu(\gamma-1) \frac{\hat{G}_{\theta\theta}}{r} \frac{\partial v_\theta}{\partial \theta} - \mu(\gamma-1) \left(\frac{2\hat{G}_{\phi\phi}}{\tan \theta} - \hat{G}_{r\theta} - \hat{G}_{\theta r} \right) \frac{v_\theta}{r} \\ \mathbf{A}_2^\phi \mathbf{v} &= \left(\gamma(p + \pi_\infty) + \frac{2\mu(\gamma-1)}{3} (\hat{G}_{rr} + \hat{G}_{\theta\theta} - 2\hat{G}_{\phi\phi}) \right) \frac{1}{r \sin \theta} \frac{\partial v_\phi}{\partial \phi} - \\ &\quad \mu(\gamma-1) \left(\frac{2\hat{G}_{\phi\phi}}{\tan \theta} - \frac{\hat{G}_{\phi\theta} + \hat{G}_{\theta\phi}}{\tan \theta} - \hat{G}_{r\phi} - \hat{G}_{\phi r} \right) \frac{v_\phi}{r} \\ \mathbf{A}_2^M \mathbf{v} &= \left[\mathbf{A}_{2,(r)}^M, \mathbf{A}_{2,(\theta)}^M, \mathbf{A}_{2,(\phi)}^M \right] \mathbf{v} = -\mu(\gamma-1) (\hat{G}_{r\theta} + \hat{G}_{\theta r}) \frac{\partial v_\theta}{\partial r} - \mu(\gamma-1) (\hat{G}_{r\phi} + \hat{G}_{\phi r}) \frac{\partial v_\phi}{\partial r} \\ &\quad - \mu(\gamma-1) (\hat{G}_{r\theta} + \hat{G}_{\theta r}) \frac{1}{r} \frac{\partial v_r}{\partial \theta} - \mu(\gamma-1) (\hat{G}_{\theta\phi} + \hat{G}_{\phi\theta}) \frac{1}{r} \frac{\partial v_\phi}{\partial \theta} \\ &\quad - \mu(\gamma-1) (\hat{G}_{r\phi} + \hat{G}_{\phi r}) \frac{1}{r \sin \theta} \frac{\partial v_r}{\partial \phi} - \mu(\gamma-1) (\hat{G}_{\phi\theta} + \hat{G}_{\theta\phi}) \frac{1}{r \sin \theta} \frac{\partial v_\theta}{\partial \phi} \end{aligned}$$

Let $\kappa = \frac{\mu c_p}{Pr}$. Then:

$$\begin{aligned} \mathbf{A}_3 f &= \mathbf{A}_3^r f + \mathbf{A}_3^\theta f + \mathbf{A}_3^\phi f = -\frac{\gamma-1}{r^2} \frac{\partial}{\partial r} \left(\kappa r^2 \frac{\partial f}{\partial r} \right) - \\ &\quad \frac{\gamma-1}{r^2 \sin \theta} \frac{\partial}{\partial \theta} \left(\kappa \sin \theta \frac{\partial f}{\partial \theta} \right) - \frac{\gamma-1}{r^2 \sin^2 \theta} \frac{\partial}{\partial \phi} \left(\kappa \frac{\partial f}{\partial \phi} \right) \\ \mathbf{B}_1 f &= \mathbf{e}_r (\mathbf{B}_1^r f) + \mathbf{e}_\theta (\mathbf{B}_1^\theta f) + \mathbf{e}_\phi (\mathbf{B}_1^\phi f) = \mathbf{e}_r \left(\frac{1}{\rho} \frac{\partial f}{\partial r} \right) + \mathbf{e}_\theta \left(\frac{1}{\rho r} \frac{\partial f}{\partial \theta} \right) + \mathbf{e}_\phi \left(\frac{1}{\rho r \sin \theta} \frac{\partial f}{\partial \phi} \right) \end{aligned}$$

Then,

$$\begin{aligned} \mathbf{B}_2 \mathbf{v} &= \mathbf{e}_r \left(\mathbf{B}_2^{r,r} \mathbf{v} + \mathbf{B}_2^{\theta,r} \mathbf{v} + \mathbf{B}_2^{\phi,r} \mathbf{v} + \mathbf{B}_2^{M,r} \mathbf{v} \right) + \\ &\quad \mathbf{e}_\theta \left(\mathbf{B}_2^{r,\theta} \mathbf{v} + \mathbf{B}_2^{\theta,\theta} \mathbf{v} + \mathbf{B}_2^{\phi,\theta} \mathbf{v} + \mathbf{B}_2^{M,\theta} \mathbf{v} \right) + \\ &\quad \mathbf{e}_\phi \left(\mathbf{B}_2^{r,\phi} \mathbf{v} + \mathbf{B}_2^{\theta,\phi} \mathbf{v} + \mathbf{B}_2^{\phi,\phi} \mathbf{v} + \mathbf{B}_2^{M,\phi} \mathbf{v} \right) \end{aligned}$$

$$\begin{aligned}
\mathbf{B}_2^{r,r} \mathbf{v} &= u_r \frac{\partial v_r}{\partial r} - \frac{1}{\rho} \left[\frac{1}{r^2} \frac{\partial}{\partial r} \left(\mu r^2 \frac{\partial v_r}{\partial r} \right) \right] - \frac{1}{3\rho} \left(\frac{\partial}{\partial r} \left[\frac{\mu}{r^2} \frac{\partial}{\partial r} (r^2 v_r) \right] \right) \\
\mathbf{B}_2^{\theta,r} \mathbf{v} &= \frac{u_\theta}{r} \frac{\partial v_r}{\partial \theta} - \frac{1}{\rho} \left[\frac{1}{r^2 \sin \theta} \frac{\partial}{\partial \theta} \left(\mu \sin \theta \frac{\partial v_r}{\partial \theta} \right) \right] \\
\mathbf{B}_2^{\phi,r} \mathbf{v} &= \frac{u_\phi}{r \sin \theta} \frac{\partial v_r}{\partial \phi} - \frac{1}{\rho} \left[\frac{1}{r^2 \sin^2 \theta} \frac{\partial}{\partial \phi} \left(\mu \frac{\partial v_r}{\partial \phi} \right) \right] \\
\mathbf{B}_2^{M,r} \mathbf{v} &= \left[\mathbf{B}_{2,(r)}^{M,r}, \mathbf{B}_{2,(\theta)}^{M,r}, \mathbf{B}_{2,(\phi)}^{M,r} \right] \mathbf{v} = -\frac{u_\theta v_\theta}{r} - \frac{u_\phi v_\phi}{r} + \frac{2\mu v_r}{\rho r^2} - 2\omega \sin \theta v_\phi \\
&\quad - \frac{1}{3\rho} \left(\frac{\partial}{\partial r} \left[\frac{\mu}{r \sin \theta} \frac{\partial}{\partial \theta} (v_\theta \sin \theta) \right] \right) - \frac{1}{3\rho} \left(\frac{\partial}{\partial r} \left[\frac{\mu}{r \sin \theta} \frac{\partial v_\phi}{\partial \phi} \right] \right) \\
&\quad - \frac{\mu}{\rho} \left[-\frac{2}{r^2 \sin \theta} \frac{\partial}{\partial \theta} (\sin \theta v_\theta) - \frac{2}{r^2 \sin \theta} \frac{\partial v_\phi}{\partial \phi} \right] - \\
&\quad - \frac{1}{\rho} \left[-\frac{2}{r^2 \sin \theta} \frac{\partial}{\partial \theta} (\mu \sin \theta v_\theta) - \frac{2}{r^2 \sin \theta} \frac{\partial (\mu v_\phi)}{\partial \phi} \right] \\
\mathbf{B}_2^{r,\theta} \mathbf{v} &= u_r \frac{\partial v_\theta}{\partial r} - \frac{1}{\rho} \left[\frac{1}{r^2} \frac{\partial}{\partial r} \left(\mu r^2 \frac{\partial v_\theta}{\partial r} \right) \right] \\
\mathbf{B}_2^{\theta,\theta} \mathbf{v} &= \frac{u_\theta}{r} \frac{\partial v_\theta}{\partial \theta} - \frac{1}{\rho} \left[\frac{1}{r^2 \sin \theta} \frac{\partial}{\partial \theta} \left(\mu \sin \theta \frac{\partial v_\theta}{\partial \theta} \right) \right] - \\
&\quad \frac{1}{3\rho} \left(\frac{1}{r^2} \frac{\partial}{\partial \theta} \left[\frac{\mu}{\sin \theta} \frac{\partial}{\partial \theta} (v_\theta \sin \theta) \right] \right) \\
\mathbf{B}_2^{\phi,\theta} \mathbf{v} &= \frac{u_\phi}{r \sin \theta} \frac{\partial v_\theta}{\partial \phi} - \frac{1}{\rho} \left[\frac{1}{r^2 \sin^2 \theta} \frac{\partial}{\partial \phi} \left(\mu \frac{\partial v_\theta}{\partial \phi} \right) \right] \\
\mathbf{B}_2^{M,\theta} \mathbf{v} &= \left[\mathbf{B}_{2,(r)}^{M,\theta}, \mathbf{B}_{2,(\theta)}^{M,\theta}, \mathbf{B}_{2,(\phi)}^{M,\theta} \right] \mathbf{v} = \frac{u_\theta v_r}{r} - \frac{u_\phi v_\phi}{r \tan \theta} + \frac{\mu v_\theta}{\rho r^2 \sin^2 \theta} - 2\omega \cos \theta v_\phi \\
&\quad - \frac{1}{3\rho} \left(\frac{1}{r^3} \frac{\partial}{\partial \theta} \left(\mu \frac{\partial (r^2 v_r)}{\partial r} \right) \right) - \frac{1}{3\rho} \left(\frac{1}{r^2} \frac{\partial}{\partial \theta} \left(\frac{\mu}{\sin \theta} \frac{\partial v_\phi}{\partial \phi} \right) \right) \\
&\quad - \frac{\mu}{\rho} \left[\frac{1}{r^2} \frac{\partial u_r}{\partial \theta} - \frac{\cos \theta}{r^2 \sin^2 \theta} \frac{\partial u_\phi}{\partial \phi} \right] - \frac{1}{\rho} \left[-\frac{1}{r^2} \frac{\partial (\mu u_r)}{\partial \theta} - \frac{\cos \theta}{r^2 \sin^2 \theta} \frac{\partial (\mu u_\phi)}{\partial \phi} \right] \\
\mathbf{B}_2^{r,\phi} \mathbf{v} &= u_r \frac{\partial v_\phi}{\partial r} - \frac{1}{\rho} \left[\frac{1}{r^2} \frac{\partial}{\partial r} \left(\mu r^2 \frac{\partial v_\phi}{\partial r} \right) \right] \\
\mathbf{B}_2^{\theta,\phi} \mathbf{v} &= \frac{u_\theta}{r} \frac{\partial v_\phi}{\partial \theta} - \frac{1}{\rho} \left[\frac{1}{r^2 \sin \theta} \frac{\partial}{\partial \theta} \left(\mu \sin \theta \frac{\partial v_\phi}{\partial \theta} \right) \right] \\
\mathbf{B}_2^{\phi,\phi} \mathbf{v} &= \frac{u_\phi}{r \sin \theta} \frac{\partial v_\phi}{\partial \phi} - \frac{1}{\rho} \left[\frac{1}{r^2 \sin^2 \theta} \frac{\partial}{\partial \phi} \left(\mu \frac{\partial v_\phi}{\partial \phi} \right) \right] - \frac{1}{3\rho} \left(\frac{1}{r^2 \sin^2 \theta} \frac{\partial}{\partial \phi} \left(\mu \frac{\partial v_\phi}{\partial \phi} \right) \right) \\
\mathbf{B}_2^{M,\phi} \mathbf{v} &= \left[\mathbf{B}_{2,(r)}^{M,\phi}, \mathbf{B}_{2,(\theta)}^{M,\phi}, \mathbf{B}_{2,(\phi)}^{M,\phi} \right] \mathbf{v} = \frac{u_\phi v_\theta}{r \tan \theta} + \frac{u_\phi v_r}{r} + \frac{\mu v_\phi}{\rho r^2 \sin^2 \theta} + 2\omega \cos \theta v_\theta + 2\omega \sin \theta v_r \\
&\quad - \frac{1}{3\rho} \left(\frac{1}{r^3 \sin \theta} \frac{\partial}{\partial \phi} \left(\mu \frac{\partial (r^2 v_r)}{\partial r} \right) \right) - \frac{1}{3\rho} \left(\frac{1}{r^2 \sin^2 \theta} \frac{\partial}{\partial \phi} \left(\mu \frac{\partial (v_\theta \sin \theta)}{\partial \theta} \right) \right) \\
&\quad - \frac{\mu}{\rho} \left[\frac{1}{r^2 \sin \theta} \frac{\partial u_r}{\partial \phi} + \frac{\cos \theta}{r^2 \sin^2 \theta} \frac{\partial u_\theta}{\partial \phi} \right] - \frac{1}{\rho} \left[\frac{1}{r^2 \sin \theta} \frac{\partial (\mu u_r)}{\partial \phi} + \frac{\cos \theta}{r^2 \sin^2 \theta} \frac{\partial (\mu u_\theta)}{\partial \phi} \right]
\end{aligned}$$

$$\mathbf{C}_2 \mathbf{v} = \mathbf{C}_2^r \mathbf{v} + \mathbf{C}_2^\theta \mathbf{v} + \mathbf{C}_2^\phi \mathbf{v} + \mathbf{C}_2^C \mathbf{v}$$

$$\begin{aligned}
\mathbf{C}_2^r \mathbf{v} &= \left((\gamma-1)T + \frac{2\mu(\gamma-1)T}{3(p+\pi_\infty)} (\hat{G}_{rr} + \hat{G}_{\theta\theta} + \hat{G}_{\phi\phi}) \right) \frac{1}{r^2} \frac{\partial (r^2 v_r)}{\partial r} - \\
&\quad 2\mu \frac{(\gamma-1)T}{p+\pi_\infty} \hat{G}_{rr} \frac{\partial v_r}{\partial r} - \mu \frac{(\gamma-1)T}{p+\pi_\infty} (2\hat{G}_{\theta\theta} + 2\hat{G}_{\phi\phi}) \frac{v_r}{r} \\
\mathbf{C}_2^\theta \mathbf{v} &= \left((\gamma-1)T + \frac{2\mu(\gamma-1)T}{3(p+\pi_\infty)} (\hat{G}_{rr} + \hat{G}_{\theta\theta} + \hat{G}_{\phi\phi}) \right) \frac{1}{r \sin \theta} \frac{\partial (\sin \theta v_\theta)}{\partial \theta} \\
&\quad - 2\mu \frac{(\gamma-1)T}{p+\pi_\infty} \frac{\hat{G}_{\theta\theta}}{r} \frac{\partial v_\theta}{\partial \theta} - \mu \frac{(\gamma-1)T}{p+\pi_\infty} \left(\frac{2\hat{G}_{\phi\phi}}{\tan \theta} - \hat{G}_{r\theta} - \hat{G}_{\theta r} \right) \frac{v_\theta}{r} \\
\mathbf{C}_2^\phi \mathbf{v} &= \left((\gamma-1)T + \frac{2\mu(\gamma-1)T}{3(p+\pi_\infty)} (\hat{G}_{rr} + \hat{G}_{\theta\theta} - 2\hat{G}_{\phi\phi}) \right) \frac{1}{r \sin \theta} \frac{\partial v_\phi}{\partial \phi} - \\
&\quad \mu \frac{(\gamma-1)T}{p+\pi_\infty} \left(\frac{2\hat{G}_{\phi\phi}}{\tan \theta} - \frac{\hat{G}_{\phi\theta} + \hat{G}_{\theta\phi}}{\tan \theta} - \hat{G}_{r\phi} - \hat{G}_{\phi r} \right) \frac{v_\phi}{r} \\
\mathbf{C}_2^M \mathbf{v} &= \left[\mathbf{C}_{2,(r)}^M, \mathbf{C}_{2,(\theta)}^M, \mathbf{C}_{2,(\phi)}^M \right] \mathbf{v} = \\
&\quad - \mu \frac{(\gamma-1)T}{p+\pi_\infty} (\hat{G}_{r\theta} + \hat{G}_{\theta r}) \frac{\partial v_\theta}{\partial r} - \mu \frac{(\gamma-1)T}{p+\pi_\infty} (\hat{G}_{r\phi} + \hat{G}_{\phi r}) \frac{\partial v_\phi}{\partial r} - \\
&\quad - \mu \frac{(\gamma-1)T}{p+\pi_\infty} (\hat{G}_{r\theta} + \hat{G}_{\theta r}) \frac{1}{r} \frac{\partial v_r}{\partial \theta} - \mu \frac{(\gamma-1)T}{p+\pi_\infty} (\hat{G}_{\theta\phi} + \hat{G}_{\phi\theta}) \frac{1}{r} \frac{\partial v_\phi}{\partial \theta} \\
&\quad - \mu \frac{(\gamma-1)T}{p+\pi_\infty} (\hat{G}_{r\phi} + \hat{G}_{\phi r}) \frac{1}{r \sin \theta} \frac{\partial v_r}{\partial \phi} - \mu \frac{(\gamma-1)T}{p+\pi_\infty} (\hat{G}_{\phi\theta} + \hat{G}_{\theta\phi}) \frac{1}{r \sin \theta} \frac{\partial v_\theta}{\partial \phi}
\end{aligned}$$

$$\mathbf{C}_3 f = \mathbf{C}_3^r f + \mathbf{C}_3^\theta f + \mathbf{C}_3^\phi f$$

$$\begin{aligned}
\mathbf{C}_3^r f &= u_r \frac{\partial f}{\partial r} - \frac{(\gamma-1)T}{(p+\pi_\infty)r^2} \frac{\partial}{\partial r} \left(\kappa r^2 \frac{\partial f}{\partial r} \right) \\
\mathbf{C}_3^\theta f &= \frac{u_\theta}{r} \frac{\partial f}{\partial \theta} - \frac{(\gamma-1)T}{(p+\pi_\infty)r^2 \sin \theta} \frac{\partial}{\partial \theta} \left(\kappa \sin \theta \frac{\partial f}{\partial \theta} \right) \\
\mathbf{C}_3^\phi f &= \frac{u_\phi}{r \sin \theta} \frac{\partial f}{\partial \phi} - \frac{(\gamma-1)T}{(p+\pi_\infty)r^2 \sin^2 \theta} \frac{\partial}{\partial \phi} \left(\kappa \frac{\partial f}{\partial \phi} \right).
\end{aligned}$$

If we denote by \mathbf{U} the vector of unknowns: $\mathbf{U} = [p, u_r, u_\theta, u_\phi, T]^T$, define \mathbf{G} as the gravity vector

$$\mathbf{G} = [0, \mathbf{g}^T, 0]^T,$$

and combine operators in corresponding directions by introducing the following block-operators:

$$\mathbf{D}_r(\mathbf{U}) = \begin{bmatrix} \mathbf{A}_1^r & \mathbf{A}_2^r & 0 & 0 & \mathbf{A}_3^r \\ \mathbf{B}_1^r & \mathbf{B}_2^{r,r} & 0 & 0 & 0 \\ 0 & 0 & \mathbf{B}_2^{r,\theta} & 0 & 0 \\ 0 & 0 & 0 & \mathbf{B}_2^{r,\phi} & 0 \\ 0 & \mathbf{C}_2^r & 0 & 0 & \mathbf{C}_3^r \end{bmatrix} \quad (4.31)$$

$$D_{\theta}(\mathbf{U}) = \begin{bmatrix} A_1^{\theta} & 0 & A_2^{\theta} & 0 & A_3^{\theta} \\ 0 & B_2^{\theta,r} & 0 & 0 & 0 \\ B_1^{\theta} & 0 & B_2^{\theta,\theta} & 0 & 0 \\ 0 & 0 & 0 & B_2^{\theta,\phi} & 0 \\ 0 & 0 & C_2^{\theta} & 0 & C_3^{\theta} \end{bmatrix} \quad (4.32)$$

$$D_{\phi}(\mathbf{U}) = \begin{bmatrix} A_1^{\phi} & 0 & 0 & A_2^{\phi} & A_3^{\phi} \\ 0 & B_2^{\phi,r} & 0 & 0 & 0 \\ 0 & 0 & B_2^{\phi,\theta} & 0 & 0 \\ B_1^{\phi} & 0 & 0 & B_2^{\phi,\phi} & 0 \\ 0 & 0 & 0 & C_2^{\phi} & C_3^{\phi} \end{bmatrix} \quad (4.33)$$

$$D_M(\mathbf{U}) = \begin{bmatrix} 0 & A_{2,(r)}^M & A_{2,(\theta)}^M & A_{2,(\phi)}^M & 0 \\ 0 & B_{2,(r)}^{M,r} & B_{2,(\theta)}^{M,r} & B_{2,(\phi)}^{M,r} & 0 \\ 0 & B_2^{M,2,(r)} & B_{2,(\theta)}^{M,r} & B_{2,(\phi)}^{M,r} & 0 \\ 0 & B_{2,(r)}^{M,r} & B_{2,(\theta)}^{M,r} & B_{2,(\phi)}^{M,r} & 0 \\ 0 & C_{2,(r)}^M & C_{2,(\theta)}^M & C_{2,(\phi)}^M & 0 \end{bmatrix} \quad (4.34)$$

the system (4.28)-(4.30) can be written in a compact form as:

$$\frac{\partial \mathbf{U}}{\partial t} + \mathbf{D}_r(\mathbf{U})\mathbf{U} + \mathbf{D}_{\theta}(\mathbf{U})\mathbf{U} + \mathbf{D}_{\phi}(\mathbf{U})\mathbf{U} + \mathbf{D}_M(\mathbf{U})\mathbf{U} + \mathbf{G} = 0. \quad (4.35)$$

References

References

- [1] S. Marras, J. Kelly, M. Moragues, A. Müller, M. Kopera, M. Vázquez, F. Giraldo, G. Houzeaux, O. Jorba, A review of element-based Galerkin methods for numerical weather prediction: Finite elements, spectral elements, and discontinuous Galerkin, *Archives of Computational Methods in Engineering* 23 (4) (2016) 673–722.
- [2] B. Fox-Kemper, A. Adcroft, C. W. Böning, E. P. Chassignet, E. Curchitser, G. Danabasoglu, C. Eden, M. H. England, R. Gerdes, R. J. Greatbatch, et al., Challenges and prospects in ocean circulation models, *Frontiers in Marine Science* 6 (2019) 65.
- [3] J. Douglas, Alternating direction methods for three space variables, *Numerische Mathematik* 4 (1) (1962) 41–63.
- [4] R. Frolov, An efficient algorithm for the multicomponent compressible navier–stokes equations in low- and high-mach number regimes, *Computers & Fluids* 178 (2019) 15–40.
- [5] H. Francis, A. Anthony, Technical report LA-4700, Tech. rep. (1971).

- [6] A. Takhirov, R. Frolov, P. Minev, A direction splitting scheme for Navier-Stokes-Boussinesq system in spherical shell geometries, ArXiv e-prints: (Feb. 2020). [arXiv:1905.02300v2](https://arxiv.org/abs/1905.02300v2).
- [7] H. P. Langtangen, Solving nonlinear ODE and PDE problems, Center for Biomedical Computing, Simula Research Laboratory and Department of Informatics, University of Oslo (2016).
- [8] C. A. Fletcher, Computational techniques for fluid dynamics. Volume 1-Fundamental and general techniques. Volume 2-Specific techniques for different flow categories, in: Berlin and New York, Springer-Verlag, 1988, p. Vol. 1, 418 p.; vol. 2, 493 p., Vol. 1, 1988.
- [9] J.-L. Guermond, P. Minev, A new class of massively parallel direction splitting for the incompressible Navier–Stokes equations, *Computer Methods in Applied Mechanics and Engineering* 200 (23) (2011) 2083–2093.
- [10] H. Guillard, C. Viozat, On the behaviour of upwind schemes in the low Mach number limit, *Computers & Fluids* 28 (1) (1999) 63–86.
- [11] P. Minev, C. R. Ethier, A characteristic/finite element algorithm for the 3-d navier–stokes equations using unstructured grids, *Computer Methods in Applied Mechanics and Engineering* 178 (1-2) (1999) 39–50.
- [12] J. Keating, Direction-splitting schemes for particulate flows, Ph.D. thesis, University of Alberta (2013).